Available online at www.sciencedirect.com

ScienceDirect

Procedia Structural Integrity 28 (2020) 411–417

Structural Integrity Procedia

www.elsevier.com/locate/procedia

1st Virtual European Conference on Fracture

Peridynamic shell membrane formulation

Erkan Oterkus[a,*], Erdogan Madenci[b], Selda Oterkus[a]

[a]*Department of Naval Architecture, Ocean and Marine Engineering, University of Strathclyde, 100 Montrose Street, Glasgow G4 0LZ, UK*
[b] *Department of Aerospace and Mechanical Engineering, The University of Arizona, 1130 N. Mountain Ave., Tucson AZ 85721, USA*

Abstract

Peridynamics (PD) is a non-local continuum theory that enables failure prediction. It enables both crack initiation and propagation as well as crack branching. Also, it has been utilized to model simplified structures such as beams, plates and shells. In this study, a new peridynamic shell membrane formulation is presented. The equations of motion are obtained by using Euler-Lagrange equations. The bond constant is determined by comparing peridynamic and classical equations of motion for shell membranes for a special condition of peridynamic internal length parameter, horizon, approaching zero. Comparison of peridynamic results with analytical results for a benchmark problem confirms the validity of the present shell membrane formulation.

Keywords: Peridynamics; Shell; Membrane; Non-local

1. Introduction

Peridynamics (PD) is a non-local continuum mechanics formulation introduced by Silling (2000). It has certain advantages with respect to some other existing methodologies especially for failure prediction. It is possible to represent both crack initiation and propagation as well as crack branching. There has been a rapid progress on peridynamics especially during the recent years. Amongst these, Basoglu et al. (2019) utilized PD to investigate micro-crack and macro-crack interactions, and how the locations and orientations of micro-cracks effect the propagation of

* Corresponding author. Tel.: +44-141-548-3876.
E-mail address: erkan.oterkus@strath.ac.uk

10.1016/j.prostr.2020.10.048

a macro-crack. Imachi et. al. (2019) developed a new concept called new transition bond and demonstrated its capability for dynamic fracture analysis. In addition, dynamic crack arrest phenomenon was studied by Imachi et. al. (2020). Kefal et. al. (2019) utilized peridynamics for topology optimization of cracked structures. Liu et. al. (2018) used peridynamics to model fracture of zigzag graphene sheets. Oterkus and Madenci (2012a,b) presented a peridynamic formulation suitable to model fiber-reinforced composites. This formulation was utilized by Oterkus et. al. (2010a) to predict damage growth from loaded composite fastener holes. Oterkus et. al. (2010b) developed a peridynamic model for fatigue analysis. In addition, Oterkus et. al. (2012) performed impact damage assessment of reinforced concrete. Vazic et. al. (2017) also investigated the micro-crack and macro-crack interactions by only considering parallel micro-cracks with respect to the macro-crack. De Meo et. al. (2016) and Zhu et. al. (2016) used peridynamics to predict granular fracture in polycrystalline materials. PD can also be used for multiphysics analysis. For example, De Meo and Oterkus (2017) simulated evolution of pitting corrosion by using peridynamics. De Meo et. al. (2017) further extended this study by examining the onset, propagation, and interaction of multiple cracks generated from corrosion pits. Diyaroglu et. al. (2017a) introduced peridynamic diffusion model and implemented in finite element framework. Moreover, Oterkus et. al. (2014) and Diyaroglu et al. (2017b) utilized PD for moisture concentration analysis which is an important concern for electronic packages. Wang et. al. (2018) utilized peridynamics to study the fracture evolution during lithiation process. An extensive review on peridynamics research is given in Madenci and Oterkus (2014) and Javili et. al. (2019).

Peridynamics has also been utilized to model simplified structures such as beams, plates and shells. Taylor and Steigmann (2015) developed a peridynamic formulation for thin plates. Yang et. al. (2020) introduced peridynamic Kirchhoff plate formulation using state-based peridynamics. O'Grady and Foster (2014a,b) derived Euler beam and Kirchhoff plate formulations within non-ordinary state-based framework. Diyaroglu et. al. (2015) proposed peridynamic Timoshenko beam and Mindlin plate formulations by taking into account transverse shear deformations. In another study, Vazic et. al. (2020) developed a peridynamic model for a Mindlin plate resting on a Winkler elastic foundation. Yang et. al. (2019) demonstrated how to implement peridynamic beam and plate formulations in finite element framework. In this study, a new peridynamic formulation is presented specifically for shell membranes. The formulation is obtained by using Euler-Lagrange equation. The formulation is compared with the classical formulation as the peridynamic length scale parameter, horizon, approaches zero. A benchmark problem is considered for validation, and peridynamic solution captures the analytical solution.

2. Peridynamic shell membrane formulation

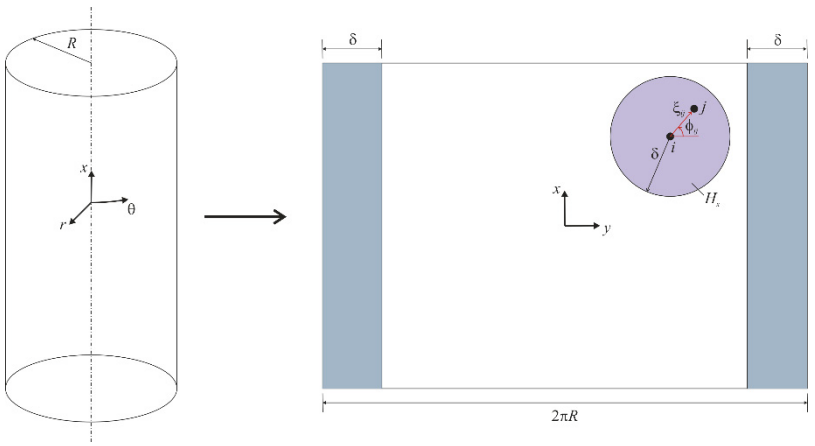

Fig. 1. Shell membrane geometry (left) and solution domain (right).

In this section, derivation of peridynamic shell membrane formulation is presented. For the geometry, a cylindrical shell membrane is considered as shown in Fig. 1. Cylindrical coordinate system is utilized by defining the coordinates; x: axial direction, θ: tangential direction and r: radial direction. To simplify the calculations, an imaginary cut is

introduced and the cylindrical domain is mapped into a 2-Dimensional domain. In the 2-Dimensional domain y -axis corresponds to tangential direction. Since the geometry is a cylinder, there should be a continuity of interactions between material points located at the left and right edges of the 2-Dimensional domain (blue regions). Each material point has three degrees of freedom; u , ϑ and w which correspond to displacement components in axial, tangential and radial directions.

To obtain the equations of motion of peridynamic shell membrane formulation, Euler-Lagrange equations are utilized as

$$\frac{d}{dt}\frac{\partial L}{\partial \dot{u}_i}-\frac{\partial L}{\partial u_i}=0 \tag{1a}$$

$$\frac{d}{dt}\frac{\partial L}{\partial \dot{\vartheta}_i}-\frac{\partial L}{\partial \vartheta_i}=0 \tag{1b}$$

$$\frac{d}{dt}\frac{\partial L}{\partial \dot{w}_i}-\frac{\partial L}{\partial w_i}=0 \tag{1c}$$

where the Lagrangian, L , is defined as

$$L=T-U \tag{2}$$

In Eq. (2), the total kinetic energy, T and total potential energy, U of the system can be expressed as

$$T=\frac{1}{2}\sum_{i=1}^{M}\rho V_i\left(\dot{u}_i^2+\dot{\vartheta}_i^2+\dot{w}_i^2\right) \tag{3a}$$

$$U=\frac{1}{2}\sum_{i=1}^{M}\sum_{j=1}^{\lambda_i}\left(\frac{c\left(\left(u_j-u_i\right)\cos\phi_{ij}+\left(\vartheta_j-\vartheta_i\right)\sin\phi_{ij}-\frac{1}{2R}\left(w_i+w_j\right)\xi_{ij}\sin^2\phi_{ij}\right)^2}{2\xi_{ij}}\right)V_jV_i-\left(b_i^u u_i+b_i^\vartheta\vartheta_i+b_i^w w_i\right)V_i \tag{3b}$$

where M is the total number of points in the solution domain, λ_i is the number of material points inside the horizon of the material point i , R is the radius of the cylinder, c is the bond constant, V is the volume of the material point, ξ_{ij} and ϕ_{ij} are the length and orientation of the bond between material points i and j , respectively. In Eq. (3b), b_i^u , b_i^ϑ and b_i^w represent body load components in axial, tangential and radial directions, respectively. By substituting Eqs. (3a,b) in Eqs. (2) and (1a-c) yields the equations of motion of the peridynamic shell membrane formulation as

$$\rho\ddot{u}_i-\sum_{j=1}^{\lambda}\left(\frac{c\left(\left(u_j-u_i\right)\cos^2\varphi_{ij}+\left(\vartheta_j-\vartheta_i\right)\sin\varphi_{ij}\cos\varphi_{ij}-\frac{1}{2R}\left(w_i+w_j\right)\xi_{ij}\sin^2\varphi_{ij}\cos\varphi_{ij}\right)}{\xi_{ij}}\right)V_j-b_i^u=0 \tag{4a}$$

$$\rho\ddot{\vartheta}_i-\sum_{j=1}^{\lambda}\left(\frac{c\left(\left(u_j-u_i\right)\sin\varphi_{ij}\cos\varphi_{ij}+\left(\vartheta_j-\vartheta_i\right)\sin^2\varphi_{ij}-\frac{1}{2R}\left(w_i+w_j\right)\xi_{ij}\sin^3\varphi_{ij}\right)}{\xi_{ij}}\right)V_j-b_i^\vartheta=0 \tag{4b}$$

$$\rho \ddot{w}_i - \sum_{j=1}^{\lambda} \left(c \left(\left(u_j - u_i \right) \cos\varphi_{ij} + \left(\vartheta_j - \vartheta_i \right) \sin\varphi_{ij} - \frac{1}{2R} \left(w_i + w_j \right) \xi_{ij} \sin^2 \varphi_{ij} \right) \left(\frac{1}{2R} \sin^2 \varphi_{ij} \right) \right) V_j - b_i^w = 0 \tag{4c}$$

The peridynamic equations of motion given in Eqs. (4a-c) can be verified by comparing them against classical equations of motion for the shell membrane for the special case of the horizon size approaches zero, i.e. $\delta \to 0$. They can be written as

$$\rho \ddot{u}_i = \frac{E}{2\left(1-\nu^2\right)} \left(2u_{i,xx} + \frac{\left(1+\nu\right)}{R} \vartheta_{i,x\theta} - \frac{2\nu}{R} w_{i,x} + \frac{\left(1-\nu\right)}{R^2} u_{i,\theta\theta} \right) + b_i^u \tag{5a}$$

$$\rho \ddot{\vartheta}_i = \frac{E}{2\left(1-\nu^2\right)} \left(\frac{\left(1+\nu\right)}{R} u_{i,x\theta} + \left(1-\nu\right) \vartheta_{i,xx} + \frac{2}{R^2} \vartheta_{i,\theta\theta} - \frac{2}{R^2} w_{i,\theta} \right) + b_i^{\vartheta} \tag{5b}$$

$$\rho \ddot{w}_i = \frac{E}{\left(1-\nu^2\right)} \left(\frac{1}{R^2} \vartheta_{i,\theta} - \frac{1}{R^2} w_i + \frac{\nu}{R} u_{i,x} \right) + b_i^w \tag{5c}$$

where ρ is density, E is elastic modulus and ν is Poisson's ratio. In Eqs. (5a-c), "dot" symbol represents derivative with respect to time whereas "comma" symbol represents derivative with respect to space.

For the horizon size converging to zero, the displacement components of the material point j can be expressed in terms of the displacement components of the material point i by using Taylor's expansion up to the second order as

$$u_j = u_i + u_{i,x} \left(x_j - x_i \right) + \frac{1}{R} u_{i,\theta} R \left(\theta_j - \theta_i \right) + \frac{1}{2!} u_{i,xx} \left(x_j - x_i \right)^2 + \frac{1}{R} u_{i,x\theta} R \left(x_j - x_i \right) \left(\theta_j - \theta_i \right) + \frac{1}{2!R^2} u_{i,\theta\theta} R^2 \left(\theta_j - \theta_i \right)^2 \tag{6a}$$

$$\vartheta_j = \vartheta_i + \vartheta_{i,x} \left(x_j - x_i \right) + \frac{1}{R} \vartheta_{i,\theta} R \left(\theta_j - \theta_i \right) + \frac{1}{2!} \vartheta_{i,xx} \left(x_j - x_i \right)^2 + \frac{1}{R} \vartheta_{i,x\theta} R \left(x_j - x_i \right) \left(\theta_j - \theta_i \right) + \frac{1}{2!R^2} \vartheta_{i,\theta\theta} R^2 \left(\theta_j - \theta_i \right)^2 \tag{6b}$$

$$w_j = w_i + w_{i,x} \left(x_j - x_i \right) + \frac{1}{R} w_{i,\theta} R \left(\theta_j - \theta_i \right) + \frac{1}{2!} w_{i,xx} \left(x_j - x_i \right)^2 + \frac{1}{R} w_{i,x\theta} R \left(x_j - x_i \right) \left(\theta_j - \theta_i \right) + \frac{1}{2!R^2} w_{i,\theta\theta} R^2 \left(\theta_j - \theta_i \right)^2 \tag{6c}$$

By using the relationships

$$x_j - x_i = \xi_{ij} \cos\phi_{ij} \tag{7a}$$

$$\vartheta_j = \vartheta_i + \vartheta_{i,x} \left(x_j - x_i \right) + \frac{1}{R} \vartheta_{i,\theta} R \left(\theta_j - \theta_i \right) + \frac{1}{2!} \vartheta_{i,xx} \left(x_j - x_i \right)^2 + \frac{1}{R} \vartheta_{i,x\theta} R \left(x_j - x_i \right) \left(\theta_j - \theta_i \right) + \frac{1}{2!R^2} \vartheta_{i,\theta\theta} R^2 \left(\theta_j - \theta_i \right)^2 \tag{7b}$$

Eqs. (6a-c) can be rewritten as

$$u_j = u_i + u_{i,x} \, \xi_{ij} \cos\phi_{ij} + \frac{1}{R} u_{i,\theta} \, \xi_{ij} \sin\phi_{ij} + \frac{1}{2!} u_{i,xx} \xi_{ij}^2 \cos^2 \phi_{ij} + \frac{1}{R} u_{i,x\theta} \xi_{ij}^2 \sin\phi_{ij} \cos\phi_{ij} + \frac{1}{2!R^2} u_{i,\theta\theta} \xi_{ij}^2 \sin^2 \phi_{ij} \tag{8a}$$

$$\vartheta_j = \vartheta_i + \vartheta_{i,x} \, \xi_{ij} \cos\phi_{ij} + \frac{1}{R} \vartheta_{i,\theta} \, \xi_{ij} \sin\phi_{ij} + \frac{1}{2!} \vartheta_{i,xx} \xi_{ij}^2 \cos^2 \phi_{ij} + \frac{1}{R} \vartheta_{i,x\theta} \xi_{ij}^2 \sin\phi_{ij} \cos\phi_{ij} + \frac{1}{2!R^2} \vartheta_{i,\theta\theta} \xi_{ij}^2 \sin^2 \phi_{ij} \tag{8b}$$

$$w_j = w_i + w_{i,x} \, \xi_{ij} \cos\phi_{ij} + \frac{1}{R} w_{i,\theta} \, \xi_{ij} \sin\phi_{ij} + \frac{1}{2!} w_{i,xx} \xi_{ij}^2 \cos^2 \phi_{ij} + \frac{1}{R} w_{i,x\theta} \xi_{ij}^2 \sin\phi_{ij} \cos\phi_{ij} + \frac{1}{2!R^2} w_{i,\theta\theta} \xi_{ij}^2 \sin^2 \phi_{ij} \tag{8c}$$

The volume of the material point *j* for an incremental volume can be expressed as

$$V_j = h \, \xi \, d\xi \, d\phi \tag{9}$$

Then, the equations of motion of the peridynamic shell membrane formulation given in Eqs. (4a-c) can be written in integral form as

$$\rho \ddot{u}_i = h\int_0^{\delta}\int_0^{2\pi}\left(\frac{c\left(\left(u_j-u_i\right)\cos^2\phi+\left(\vartheta_j-\vartheta_i\right)\sin\phi\cos\phi-\frac{1}{2R}\left(w_i+w_j\right)\xi\sin^2\phi\cos\phi\right)}{\xi}\right)\xi\, d\xi\, d\phi \tag{10a}$$

$$\rho \ddot{\vartheta}_i = h\int_0^{\delta}\int_0^{2\pi}\left(\frac{c\left(\left(u_j-u_i\right)\sin\phi\cos\phi+\left(\vartheta_j-\vartheta_i\right)\sin^2\phi-\frac{1}{2R}\left(w_i+w_j\right)\xi\sin^3\phi\right)}{\xi}\right)\xi\, d\xi\, d\phi \tag{10b}$$

$$\rho \ddot{w}_i = h\int_0^{\delta}\int_0^{2\pi}\left(c\left(\left(u_j-u_i\right)\cos\phi+\left(\vartheta_j-\vartheta_i\right)\sin\phi-\frac{1}{2R}\left(w_i+w_j\right)\xi\sin^2\phi\right)\left(\frac{1}{2R}\sin^2\phi\right)\right)\xi\, d\xi\, d\phi \tag{10c}$$

After substituting Eqs. (8a-c) in Eqs. (10a-c) and performing integrations result in

$$\rho \ddot{u}_i = \frac{c\,h\,\pi\,\delta^3}{16}\left(2u_{i,xx}+\frac{2}{3R^2}u_{i,\theta\theta}+\frac{4}{3R}\vartheta_{i,x\theta}-\frac{2}{3R}w_{i,x}\right) \tag{11a}$$

$$\rho \ddot{\vartheta}_i = \frac{c\,h\,\pi\,\delta^3}{16}\left(\frac{4}{3R}u_{i,x\theta}+\frac{2}{3}\vartheta_{i,xx}+\frac{2}{R^2}\vartheta_{i,\theta\theta}-\frac{2}{R^2}w_{i,\theta}\right) \tag{11b}$$

$$\rho \ddot{w}_i = \frac{c\,h\,\pi\,\delta^3}{8}\left(\frac{1}{R^2}\vartheta_{i,\theta}-\frac{1}{R^2}w_i+\frac{1}{3R}u_{i,x}\right) \tag{11c}$$

Please note that the equations of motion obtained from peridynamics given in Eqs. (11a-c) have the same form as the classical equations of motion given in Eqs. (5a-c). By equating Eqs. (11a-c) and (5a-c) yields the following relationships

$$c = \frac{9E}{\pi\,h\,\delta^3} \tag{12a}$$

and

$$\nu = \frac{1}{3} \tag{12b}$$

3. Numerical results

In order to validate the current peridynamic shell membrane formulation, an isotropic cylindrical shell having 1m edge length, 0.1592 m radius and 0.01 m thickness is considered. The elastic modulus and Poisson's ratio are specified as 200 GPa and 1/3, respectively. As shown in Fig. 1, the cylindrical shell geometry is mapped into a 2-Dimensional domain for numerical solution. For spatial discretization, a discretization size of $\Delta = 0.01\,\mathrm{m}$ is utilized. The horizon size size is chosen as $\delta = 3\Delta$. The steady-state solution is obtained by using adaptive dynamic relaxation scheme presented in Kilic and Madenci (2010). A uni-axial loading condition in the *x*-direction is applied as a body load with an amount of 5×10^9 N/m^3 along a region of $0.04\,\mathrm{m}$ at the top and bottom edges. Since the 2-Dimensional domain is used for the numerical solution of the cylindrical shell, an additional condition is enforced so that the material points at the left and right edges of the solution domain inside a region with a thickness of horizon size interact with each other.

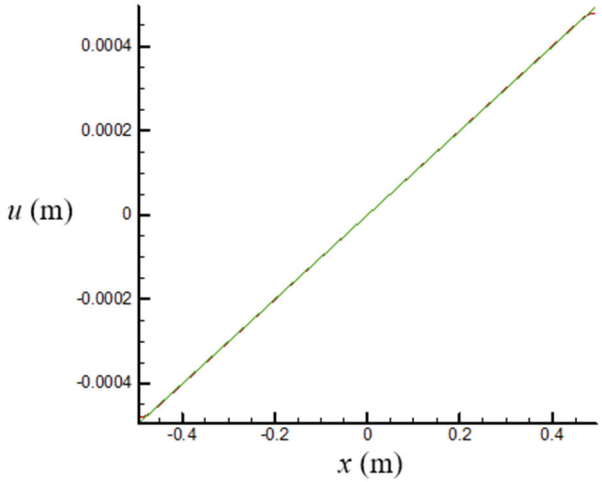

Fig. 2. Variation of axial displacements along the axial direction (Red: PD, Green: Analytical).

Variation of axial displacements along the axial direction and radial displacements along the tangential direction are shown in Figs. 2 and 3, respectively. PD results are compared against the analytical solutions and a very good agreement is observed between the two solutions.

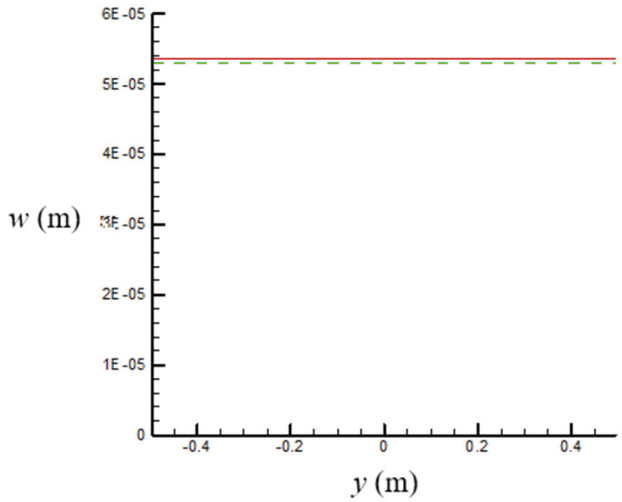

Fig. 3. Variation of radial displacements along the tangential direction (Red: PD, Green: Analytical).

4. Conclusions

In this study, a new peridynamic formulation was presented for shell membranes. Peridynamic equations were obtained by using Euler-Lagrange equations. The bond constant expression was determined by comparing peridynamic equations of motion against classical equations of motion for a special case of horizon converging to zero. To validate the newly developed peridynamic formulation, a cylindrical shell membrane subjected to tension loading was considered. Peridynamic results were compared against finite element analysis solutions and a very good agreement was observed between the two solutions.

References

Basoglu, M.F., Zerin, Z., Kefal, A., Oterkus, E., 2019. A computational model of peridynamic theory for deflecting behavior of crack propagation with micro-cracks. Computational Materials Science 162, 33–46.
De Meo, D., Zhu, N., Oterkus, E., 2016. Peridynamic modeling of granular fracture in polycrystalline materials. Journal of Engineering Materials and Technology 138(4), 041008.
De Meo, D., Oterkus, E., 2017. Finite element implementation of a peridynamic pitting corrosion damage model. Ocean Engineering 135, 76–83.
De Meo, D., Russo, L., Oterkus, E., 2017. Modeling of the onset, propagation, and interaction of multiple cracks generated from corrosion pits by using peridynamics. Journal of Engineering Materials and Technology 139(4), 041001.
Diyaroglu, C., Oterkus, E., Oterkus, S., Madenci, E., 2015. Peridynamics for bending of beams and plates with transverse shear deformation. International Journal of Solids and Structures, 69, 152–168.
Diyaroglu, C., Oterkus, S., Oterkus, E., Madenci, E., 2017. Peridynamic modeling of diffusion by using finite-element analysis. IEEE Transactions on Components, Packaging and Manufacturing Technology 7(11), 1823–1831.
Diyaroglu, C., Oterkus, S., Oterkus, E., Madenci, E., Han, S., Hwang, Y., 2017. Peridynamic wetness approach for moisture concentration analysis in electronic packages. Microelectronics Reliability 70, 103–111.
Diyaroglu, C., Oterkus, E., Oterkus, S., 2019. An Euler–Bernoulli beam formulation in an ordinary state-based peridynamic framework. Mathematics and Mechanics of Solids 24(2), 361–376.
Imachi, M., Tanaka, S., Bui, T.Q., Oterkus, S., Oterkus, E., 2019. A computational approach based on ordinary state-based peridynamics with new transition bond for dynamic fracture analysis. Engineering Fracture Mechanics 206, 359–374.
Imachi, M., Tanaka, S., Ozdemir, M., Bui, T.Q., Oterkus, S., Oterkus, E., 2020. Dynamic crack arrest analysis by ordinary state-based peridynamics. International Journal of Fracture 221(2), pp.155–169.
Javili, A., Morasata, R., Oterkus, E., Oterkus, S., 2019. Peridynamics review. Mathematics and Mechanics of Solids 24(11), 3714-3739.
Kefal, A., Sohouli, A., Oterkus, E., Yildiz, M., Suleman, A., 2019. Topology optimization of cracked structures using peridynamics. Continuum Mechanics and Thermodynamics 31(6), 1645–1672.
Kilic, B., Madenci, E., 2010. An adaptive dynamic relaxation method for quasi-static simulations using the peridynamic theory. Theoretical and Applied Fracture Mechanics 53(3), 194–204.
Liu, X., He, X., Wang, J., Sun, L., Oterkus, E., 2018. An ordinary state-based peridynamic model for the fracture of zigzag graphene sheets. Proceedings of the Royal Society A: Mathematical, Physical and Engineering Sciences 474(2217), p.20180019.
Madenci, E., Oterkus, E., 2014. Peridynamic theory. Springer, New York, NY.
O'Grady, J., Foster, J., 2014a. Peridynamic beams: a non-ordinary, state-based model. International Journal of Solids and Structures 51(18), 3177–3183.
O'Grady, J. and Foster, J., 2014b. Peridynamic plates and flat shells: A non-ordinary, state-based model. International Journal of Solids and Structures, 51(25-26), 4572–4579.
Oterkus, E., Barut, A., Madenci, E., 2010a. Damage growth prediction from loaded composite fastener holes by using peridynamic theory. In 51st AIAA/ASME/ASCE/AHS/ASC Structures, Structural Dynamics, and Materials Conference 18th AIAA/ASME/AHS Adaptive Structures Conference, Orlando, Florida, USA, p. 3026.
Oterkus, E., Guven, I. and Madenci, E., 2010b. Fatigue failure model with peridynamic theory. In 12th IEEE Intersociety Conference on Thermal and Thermomechanical Phenomena in Electronic Systems, Las Vegas, Nevada, USA, p. 1-6.
Oterkus, E., Madenci, E., 2012a. Peridynamics for failure prediction in composites. In 53rd AIAA/ASME/ASCE/AHS/ASC Structures, Structural Dynamics and Materials Conference 20th AIAA/ASME/AHS Adaptive Structures Conference, Honolulu, Hawaii, USA, p. 1692.
Oterkus, E., Madenci, E., 2012b. Peridynamic theory for damage initiation and growth in composite laminate. Key Engineering Materials 488, 355–358.
Oterkus, E., Guven, I., Madenci, E., 2012. Impact damage assessment by using peridynamic theory. Open Engineering 2(4), 523–531.
Oterkus, S., Madenci, E., Oterkus, E., Hwang, Y., Bae, J., Han, S., 2014, May. Hygro-thermo-mechanical analysis and failure prediction in electronic packages by using peridynamics. In 2014 IEEE 64th Electronic Components and Technology Conference (ECTC), Orlando, Florida, USA, p. 973-982.
Silling, S.A., 2000. Reformulation of elasticity theory for discontinuities and long-range forces. Journal of the Mechanics and Physics of Solids 48(1), 175–209.
Taylor, M., Steigmann, D.J., 2015. A two-dimensional peridynamic model for thin plates. Mathematics and Mechanics of Solids 20(8), 998–1010.
Vazic, B., Wang, H., Diyaroglu, C., Oterkus, S., Oterkus, E., 2017. Dynamic propagation of a macrocrack interacting with parallel small cracks. AIMS Materials Science 4(1), pp.118–136.
Vazic, B., Oterkus, E., Oterkus, S., 2020. Peridynamic model for a Mindlin plate resting on a Winkler elastic foundation. Journal of Peridynamics and Nonlocal Modeling, pp.1–10.
Wang, H., Oterkus, E., Oterkus, S., 2018. Predicting fracture evolution during lithiation process using peridynamics. Engineering Fracture Mechanics 192, 176–191.
Yang, Z., Oterkus, E., Nguyen, C.T., Oterkus, S., 2019. Implementation of peridynamic beam and plate formulations in finite element framework. Continuum Mechanics and Thermodynamics 31(1), 301–315.
Yang, Z., Vazic, B., Diyaroglu, C., Oterkus, E., Oterkus, S., 2020. A Kirchhoff plate formulation in a state-based peridynamic framework. Mathematics and Mechanics of Solids 25(3), 727–738.
Zhu, N., De Meo, D., Oterkus, E., 2016. Modelling of granular fracture in polycrystalline materials using ordinary state-based peridynamics. Materials 9(12), p.977.